



— IF-UFRJ-92-25 —

# INSTITUTO DE FÍSICA -



IF/UFRJ/92/25

RAYLEIGH SCATTERING FROM  
CRYSTALS AND AMORPHOUS STRUCTURES

O.D. Gonçalves, W.M.S. Santos, J. Eichler  
and  
A.M. Borges

Sept/92

LIBRARY

0161 1992

UNIVERSIDADE FEDERAL DO RIO DE JANEIRO  
INSTITUTO DE FÍSICA  
Cx. P. 68528  
21.944 - RIO DE JANEIRO  
BRASIL

# RAYLEIGH SCATTERING FROM CRYSTALS AND AMORPHOUS STRUCTURES

O.D.Gonçalves, W.M.S.Santos

*Instituto de Física da UFRJ, C.Postal 68528, Rio de Janeiro, CEP 21941, RJ Brazil*

J.Eichler

*Technische Fachhochschule Berlin, Physiklabor, 1000 Berlin 65, Germany*

A.M.Borges

*Instituto de Física da UFF, C.Postal 100296, Niteroi, CEP 24020, RJ Brazil*

## ABSTRACT

Elastic scattering cross sections of photons for momentum transfer in the range  $0.1\text{\AA}^{-1} \leq x \leq 2.2\text{\AA}^{-1}$  with  $E\gamma = 59.5$  and  $316$  keV, were measured in order to test the limits of momentum transfer within which the scattering can be considered as being due to free atoms (Rayleigh Scattering). Polycrystalline aggregate, liquid, perfect single crystals and crystal powder samples were used as scatterers. The measurements for  $E\gamma = 316$  keV and  $59.5$  keV were carried out in the angular ranges  $\theta = 0.5^\circ - 10^\circ$  and  $2^\circ - 23^\circ$  with a geometrical resolution of  $0.1^\circ$  and  $1^\circ$ , respectively. At the present time, most of the precise experimental data on elastic photon scattering have been measured using solid molecular structures as scatterers. The present results allow the conclusion that high precise data ( $\Delta d\sigma/d\Omega \leq 2\%$ ) on elastic scattering of photons can be compared with Rayleigh scattering theories only for  $x > 2\text{\AA}^{-1}$ .

## INTRODUCTION

Elastic scattering of photons is an important process to obtain information about atomic wave functions and structures, to test perturbational theories and associated computational methods.

These data are important in many interdisciplinary problems where the information about the interaction between photons and matter plays a very important role. From the

solid state point of view, an accurate knowledge of the interaction between photons and free atoms is required for understanding interference effects due to molecular structures.

In the low energy range, under  $100$  keV and near the absorption edges, the elastic scattering process (known as *anomalous scattering*) is particularly important due to the strong variation of the scattering cross section with the incident photon energy.

Many experiments were performed in order to measure the elastic cross section and many of them were compared with Rayleigh scattering theories<sup>1</sup>, where it is assumed that the atoms are free.

In a former work<sup>2</sup> we have reported the occurrence of interference effects in photon scattering by polycrystalline aggregate due to Bragg scattering. It was shown that for low momentum transfer ( $x \leq 2\text{\AA}^{-1}$ ), where:

$$x = (E/12.398) * \sin(\theta/2)$$

E= energy of the incident photon in keV

$\theta$  = scattering angle

the scattering cannot be explained as being due to free atoms. Otherwise, for higher momentum transfer, it was verified that the coherence of the photons scattered by different atoms decreases, destroying the information about the molecular structure which makes the free atom approximation applicable.

In another work<sup>3</sup> it was shown that interference effects in solids are due to Thermal Diffuse Scattering (TDS) and that there are limits above which it is possible to approximate scattering as being due to free atoms (Rayleigh scattering). In this case, experimental data are very well described by second order perturbation theories<sup>4</sup> or, in some cases, by form factor theories<sup>9,10</sup>.

In this work, we intend to study other structures and check the energy dependence of the scattering process.

## EXPERIMENTAL PROCEDURE

Two experiments were performed depending on the photon energy used.

The first experiment was performed at the Nuclear Physics Department of the Universidade Federal do Rio de Janeiro. The relative elastic scattering differential cross section  $(d\sigma/d\Omega)_{rel}$  was measured for polycrystalline aggregate (Pb and Si), for a perfect crystal (Si) and for a liquid sample (Hg). The experimental set up is the same described in reference<sup>2</sup> using an Americium gamma source ( $Am^{241}$ ,  $E\gamma = 59.5$  keV,  $I = 100$  mCi). The polycrystalline samples used were lead (  $0.137$  g/cm<sup>2</sup> ) and silicon crystal powder (  $1.196$  g/cm<sup>2</sup> ). The perfect crystal was Si (  $3.215$  g/cm<sup>2</sup> ). Mercury (  $0.487$  g/cm<sup>2</sup> ), inside a plexiglass capsule  $0.25$  mm thick, was used as the liquid sample.

The second experiment was performed at the Hahn-Meitner Institut of Berlin, with a strong Iridium gamma source ( $Ir^{248}$ ,  $E\gamma = 316$  keV,  $I = 50$  Ci). The experimental setup is similar to that used at  $59.5$  keV, but with much higher geometric accuracy ( $0.1^0$ ) (described elsewhere<sup>6</sup>). The targets used were a polycrystalline aggregate (Pb,  $3.40$  g/cm<sup>2</sup>), a perfect crystal (Si,  $4.66$  g/cm<sup>2</sup>) and a liquid sample, which consisted of  $2.70$  g/cm<sup>2</sup> of Hg, in a glass capsule  $1.0$  mm thick.

The results for the liquid samples are corrected by subtracting the contributions for the scattered photon intensity due to the capsule material, which was measured separately.

## RESULTS

The experimental results are presented in fig 1 to 3.

The results are compared with theoretical calculations which include Compton and Rayleigh scattering cross sections. The Compton cross sections were obtained from the incoherent scattering functions<sup>9</sup>, while the Rayleigh cross sections were obtained from the form-factor<sup>9</sup> approximation, or performed by Kissel<sup>8</sup> using the second order perturbation theory.

Since we are interested in relative differential cross section, this was obtained from:

$$d\sigma/d\Omega_{rel} = N(Z, E, \Omega, \theta) * \frac{1}{F_{att}}(Z, \theta_i, \theta_s)$$

where,

$N(Z, E, \Omega, \theta)$  is the count rate of the scattered radiation.

$\frac{1}{F_{att}}(Z, \theta_i, \theta_s)$  is the correction for  $\gamma$  attenuation for both incident and scattered beam.

For normal incidence ( $\theta_i = 90^0$ ) and  $\theta = \theta_s$ ,  $\frac{1}{F_{att}}$  is given by:

$$\frac{1}{F_{att}} = \frac{(e^{-\mu a} - e^{-\mu a/\cos\theta_s})}{a\mu(1 - 1/\cos\theta_s)}$$

$a$  = sample thickness in g/cm<sup>2</sup>

$\mu$  = total attenuation coefficient in cm<sup>2</sup>/g.

The error associated with the experimental momentum transfer is given by:

$$\delta x = A\{[(E/2)\cos(\theta/2)\delta\theta]^2 + [\sin(\theta/2)\delta E]^2\}^{1/2}$$

where  $E$  is the photon energy,  $\theta$  the scattering angle, and  $A = (1/12.398)(\text{\AA}^{-1} \cdot keV^{-1})$ .

For both photon energies ( $316$  keV and  $59.54$  keV) the resulting momentum transfer accuracies have the same order of magnitude ( $0.1$  and  $0.2 \text{\AA}^{-1}$ ), which makes possible a direct comparison between both experimental data. In order to compare measured and theoretical data, and since the obtained experimental data are relative cross sections, it was necessary to multiply the theoretical values by a normalization factor obtained from:

$$C = \left[ \frac{d\sigma(\alpha)}{d\Omega} \right]_{exp} * \left[ \frac{d\sigma(\alpha)}{d\Omega}_{rayleigh} + \frac{d\sigma(\alpha)}{d\Omega}_{compton} \right]_{theoretical}^{-1}$$

where  $\alpha$  is a chosen scattering angle in a region where no interference effects were expected.

In the considered range of momentum transfer ( $0.05$  and  $2.0 \text{\AA}^{-1}$ ) the maximum Compton shift is  $1.0$  keV for  $59.5$  keV and  $3.0$  keV for  $316$  keV, which does not allow to distinguish the elastic from the inelastic process. For Pb and Hg the maximum contribution from Compton to scattered amplitude is  $7\%$ , while for silicon it rises up to  $70\%$ .

a) Polycrystalline aggregate and crystal powder

Metal structures and crystal powder are similar in describing the scattering process. As reported early for metals, the observed oscillations are due to interference effects ( Bragg peaks) convoluted with the geometrical accuracy of the experimental set up<sup>2</sup>.

The measurement with lead, already reported <sup>2</sup>, was repeated in order to control the experimental conditions and also to compare the results with the new 316 keV data.

The results for Pb and Si are presented in fig 1 and 3. In fig 1 it is possible to notice that for lead and  $x \geq 0.5 \text{ \AA}^{-1}$  the experimental data show a good agreement with both calculations. Also for silicon powder (fig 3), it is possible to notice that depending on the desired accuracy, the free atom model could be used to describe the experimental data for  $x \geq 0.5 \text{ \AA}^{-1}$

#### b) Perfect crystals

The experiment performed with the perfect single crystal of Si, was done trying to avoid the Bragg conditions. This was done by fixing the incidence angle in  $90^\circ$ . In this case the interference between the elastic scattered photon is expected to be destructive, and no elastic scattered photon should be detected.

Owing to the angular divergence of the beam, the Bragg diffraction could not always be avoided, resulting in diffraction peaks for  $x = .53$  and  $.67 \text{ \AA}^{-1}$  for 316 keV and peaks for  $x = .26$ ,  $.53$  and  $.83 \text{ \AA}^{-1}$  for 59.5 keV (fig.3) . For the corresponding scattering angles, a new data set was measured rotating the crystal in order to avoid the Bragg conditions. As expected, the scattered intensities were drastically reduced (points marked as  $\Delta$  in fig.3).

From the experimental results for Si, it is possible to say that the free atom approximation applies for  $x \geq 1.0 \text{ \AA}^{-1}$ . The remaining scattered photon intensity is due to Compton scattering and to thermal diffuse scattering (TDS) and this procedure can be used as a new way to measure these two effects.

#### c) Amorphous structure (liquid)

In figure 2, it is shown the results for mercury ( 59.54 and 316 keV). As described in <sup>7</sup> the interference effect in this case is due to a molecular correlation which represents a mean distance between the molecules. It implies that the obtained interference peaks do not depend on the geometrical resolution. As in the metals, the more the momentum transfer, grows the more the thermal motion of the molecules will grow, i.e., the scattering process approaches to the free atom model. In fig 2 , it is possible to observe that the limit for mercury lies around  $0.6 \text{ \AA}^{-1}$ .

### CONCLUSIONS

The agreement between both data set on both energies are very good, confirming that momentum transfer is a good choice to scale the dependence of the scattered photon intensity with angle and energy in low momentum transfer range.

From the two experimental data sets it is possible to conclude that, for each atomic structure there are limits above which the free atom approximation applies. This limit depends on the temperature, on the molecular structure and on the experimental resolution <sup>3</sup>. In the present work it was found that for  $x$  greater than  $1.0 \text{ \AA}^{-1}$  no more oscillations were detected when considering an experimental resolution of about  $0.1 \text{ \AA}^{-1}$ .

Due to the complex dependence of the interference process on temperature and experimental setup, and due to the impossibility of knowing most of the molecular structure with the necessary accuracy, it is impossible to predict the exact limits for which the free model applies. Since within 10% no oscillation were detected for  $x$  greater than  $1.0 \text{ \AA}^{-1}$ , we suggest that, for grant,  $2.0 \text{ \AA}^{-1}$  could be taken as the limit. For more accuracy a careful angular systematic should be done in each considered case.

## ACKNOWLEDGEMENTS

We would like to express our thanks to Dr. Wolfgang Jauch for providing access to the HMI spectrometer facilities and to Andreas Palmer for his kind helpfulness. We would also like to thank to Dr. C. Cusatis and Dr. I. Mazzaro for providing helpful discussions. We are also grateful to Dr. L. Kissel for performing the theoretical calculations, as well as for the careful revision of this paper. We are also indebted to the Deutch Academic Austausch Dienst (DAAD) for supporting the travel costs to German, and to the Brazilian agencies CNPq, FAPERJ and FINEP for supporting the Brazilian part of the work.

## References

- 1) O.D. Gonçalves, I. Mazzaro and C. Cusatis, IRPS-News, **4** (1990) 9
- 2) J. Eichler, O.D. Gonçalves and S. de Barros, Phys. Rev., **A37** (1988) 3702
- 3) O.D. Gonçalves, C. Cusatis and I. Mazzaro, to be published
- 4) L. Kissel and R.H. Pratt, Phys. Rep., **140** (1986) 75
- 5) O.D. Gonçalves, S. de Barros and J. Eichler, Nucl. Instr. Meth, **A280**, (1989) 375
- 6) J.R. Schneider, J. Cryst. Growth, **65** (1983) 660
- 7) R. Kaplow, S.L.S. Strong and B.L. Averbach, Phys. Rev., **138A** (1965) 1336
- 8) L. Kissel, private communication.
- 9) J.H. Hubbel et al, J. Phys. Chem. Ref. Data, **4** (1975) 471
- 10) D. Schaupp et al, J. Phys. Chem. Ref. Data, **12** (1983) 467

## FIGURE CAPTIONS

- FIG 1.** Comparison between experimental scattering cross sections (circles) for Pb with 59,5 and 316 keV  $\gamma$  rays and free atom scattering theories. Theoretical curves were obtained from form-factor approximation (solid lines) and second order perturbation theory<sup>8</sup> (dashed lines) added to the Compton cross sections obtained from S factor. The dashed line binding experimental points are only a guide to the eye. Experimental errors ( $\leq 7\%$ ) are smaller than the point size.
- FIG 2.** The same as FIG 1 for Hg. It was not included the second order perturbation theory curve.
- FIG 3.** Comparison between experimental scattering cross sections and theory for silicon perfect crystals (59,5 and 316 keV) and for silicon powder (59,5 keV). Theoretical curve (solid line) are Rayleigh + Compton cross sections obtained with form factor and S factor respectively. Dashed lines: Compton cross sections

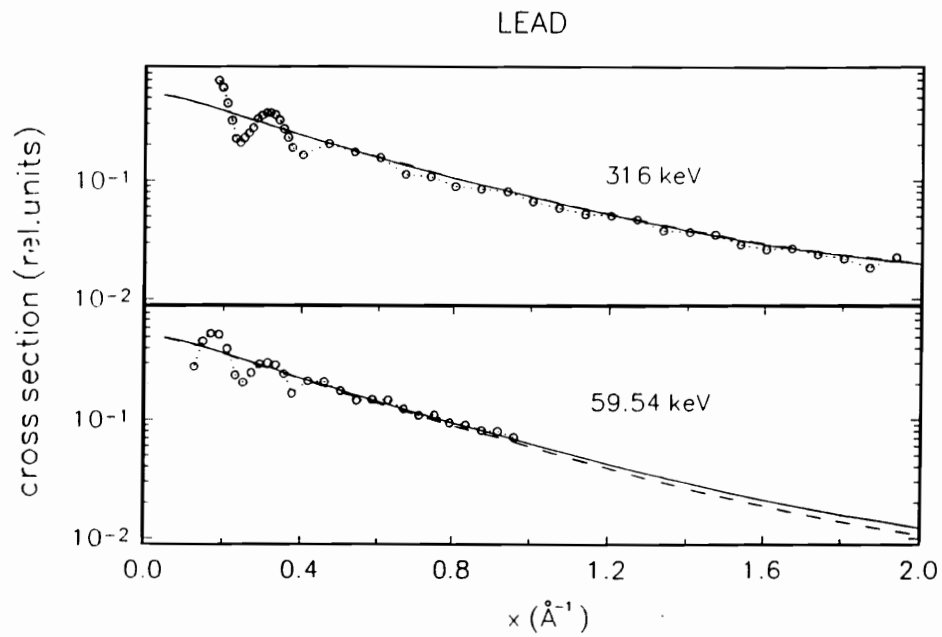


Fig. 1

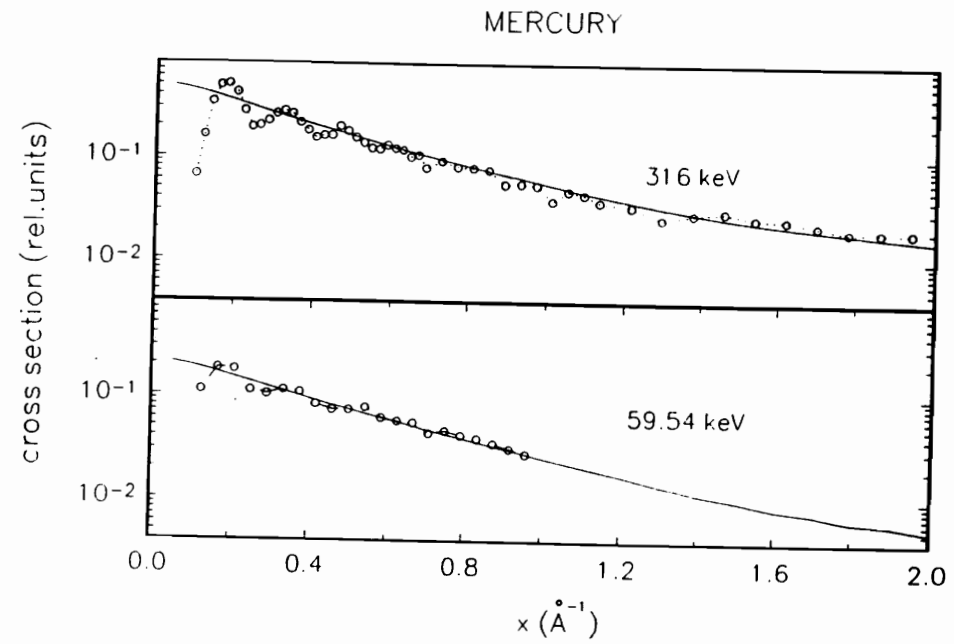


Fig. 2

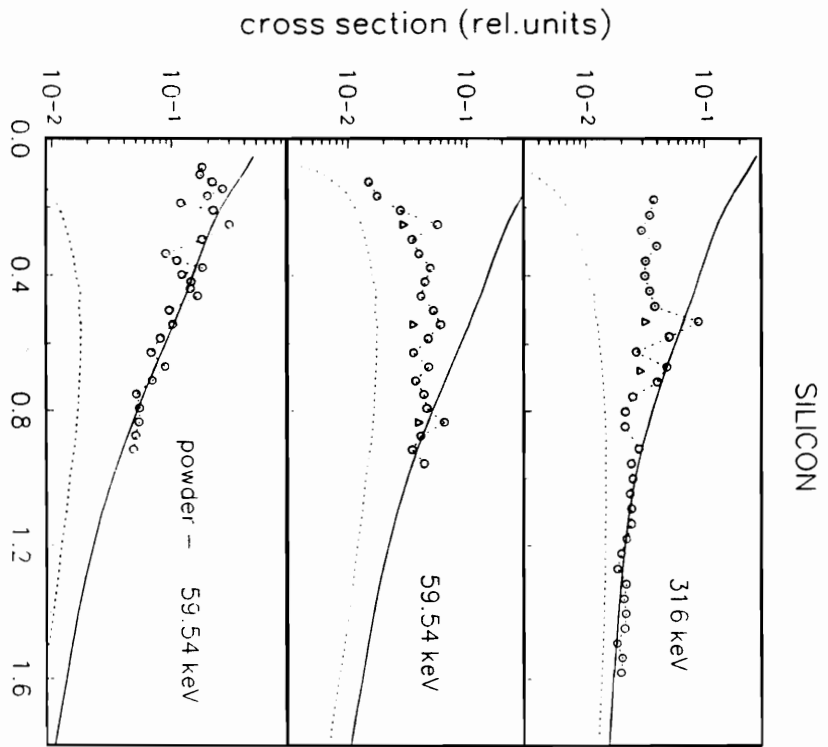


Fig 3